High Speed Maritime Ship-to-Ship/Shore Mesh Networks

Jaya Shankar Pathmasuntharam[1], Joe Jurianto[1], Peng-Yong Kong[1], Yu Ge[1], Mingtou Zhou[2], Ryu Miura[2]

[1]Network Technology Department, Institute for Infocomm Research, 21 Heng Mui Keng Terrace, Singapore 119613.

[2]Wireless Communications Laboratory, National Institute of Information and Communication Technology (NICT), 20 Science Park Road, #01-08A/10 TeleTech Park, Singapore 117674.

jshankar@i2r.a-star.edu.sg

***Abstract*—This paper gives an overview of the TRITON project that aims to develop a high-speed maritime ship-to-ship/shore mesh network. We present the general architecture of the TRITON system and detail our preliminary studies and findings that will help us determine the feasibility of using ships and shoreline base stations to form a mesh network.**

Keywords - component, Maritme, Mesh Networks, Ship-to-ship communications.

I. Introduction

Current maritime communication systems are based on narrowband UHF and VHF radios for ship-to-shore communications near port waters and satellite communication for long-range ship-to-ship and ship-to-shore communications. Legacy UHF and VHF radios are low bandwidth radios that are incapable of supporting bandwidth hungry applications. The bandwidth of satellite system such as INMARSAT's Fleet system [1] is also low when compared to land-based wireless systems such as 3G and they provide only up to 64 kbps of data bandwidth per-link. This link throughput drops when there is sharing between nodes. The future INMARSAT's BGAN system is expected to provide up to 492 kbps data bandwidth. However, the cost of satellite equipment and bandwidth for such a network is expected to remain high due to the cost of antenna stabilizers and cost of launching satellites into orbit, respectively.

The TRITON project aims to develop a ship-to-ship/shore mesh network that provides an alternative high speed communication system that can operate reasonably well in busy shipping lanes, narrow water channels and traffic lanes close to shorelines. Due to the larger expected bandwidth, newer applications such as video surveillance for piracy prevention, real time updates on navigational data, etc. can be supported on this network. Some of these newly envisaged applications will demand a strict network quality of service (OoS) such as significantly higher bandwidth and lower delays. For the mesh network to work, some of the most stringent operational requirements have to be resolved first. Building the mesh network in the sea will be challenging because there is a certain degree of uncontrolled dynamism causing weak and episodic communication that is due to propagation of RF over waters, multi-path due to surface reflection, wave occlusion, blockage of RF signal due to large metal bodies and wave rocking motion (pitch, roll and yaw).

The work on TRITON ship-to-ship/shore mesh networks is still an ongoing effort and this paper presents some of the studies and ongoing works that we have carried out in the project. In Section 2, we discuss the general architecture of the TRITON network, which is based on meshing the radios on board the ships, land stations and buoys. In Section 3, we study the feasibility of communicating between the land station and ship, and between ship to ship through empirical measurements of the radio propagation characteristics in a typical maritime communication environment. In Section 4, we present initial studies on the feasibility of forming a wireless multi-hop network among ships after analyzing the network connectivity among these ships based on their actual mobility traces derived from automatic identification system (AIS) data. In Section 5, we study the mobility pattern of the ships that passes through the Singapore Straits. The efforts highlighted in Sections 3, 4 and 5 will be eventually used to facilitate the design of a maritime simulator, which is briefly described in Section 6. The maritime simulator will be used to design and evaluate a suite of networking protocol schemes to provide robust and efficient end-to-end QoS in the wireless mesh network.

II. Architecture

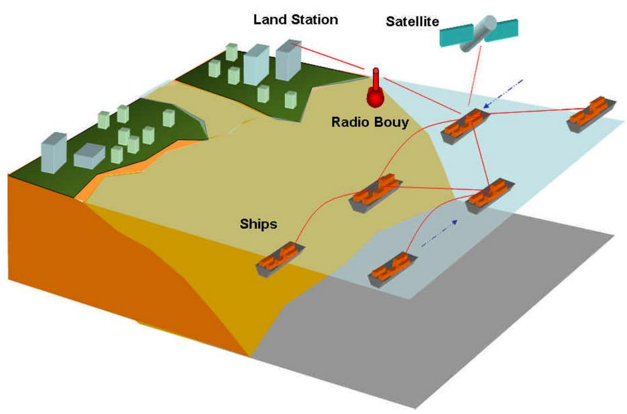

Figure 1. The high level architecture of TRITON

The high level architecture of TRITON is illustrated in Figure 1. In TRITON, the coverage extension is achieved by forming a wireless multi-hop network amongst neighboring ships, marine beacons and buoys. The multi-hop wireless

1-4244-1178-5/07/$25.00 ©2007 IEEE.

network will be connected to the terrestrial networks via land stations, which are placed at regular intervals along the shoreline. The TRITON network resembles a vehicular ad hoc network (VANET) based on cars but with some unique characteristics given by the distinct ship mobility pattern, position awareness of neighboring ships via the AIS, wave rocking movement and wave occlusion due to sea surface.

Each ship will carry a mesh radio that has the capability of frequency agility where frequencies can be switched to suite the geographic location or sea conditions. In port waters or narrow water channels, the radio frequency usage will be based on radio frequencies that are limited by land based terrestrial communication systems. Example frequencies of interest are 5.8 GHz or 2.4 GHz ISM bands. In locations far away from land, the frequencies could be in UHF, VHF or HF bands. While the mesh system is ideal when there are sufficient ships to relay the transmission, in locations where ships are sparse, the TRITON system can fall back to the satellite communication link. In our current architecture, we include a switching middleware that automatically switches the link based on the quality of links available. To realise the mesh radio, we are using the IEEE 802.16 mesh and IEEE 802.16e standards.

III. Path Loss Measurement and WiMAX performance

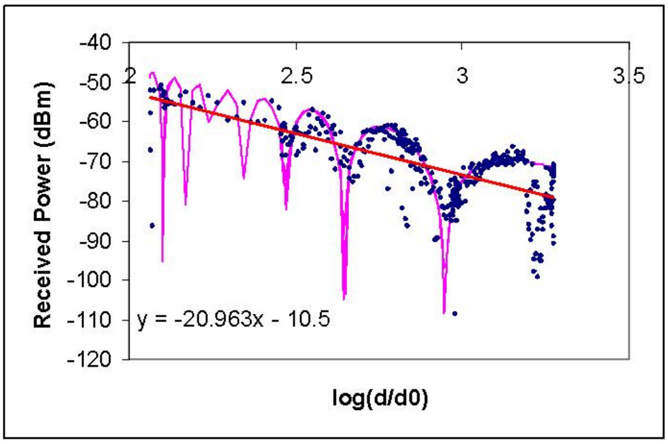

Figure 2. Received power vs. log of normalized distance for TX at 76 m

There have been many studies conducted to evaluate the propagation of radio in urban environment and the derived models are well covered in [2]. However, there are very few efforts to study propagation over sea water. The propagation characteristics in the sea have been reported to be quite different from the land. J. An [3] have analyzed maritime propagation at 1.8 GHz and focused on small-scale path loss measurements. In [4] and [5], we have carried out a series of experiment to investigate the large-scale path loss measurements at 5.8 GHz and performance measurement of WiMAX in the 5.8 GHz band. More recently, we have also carried out experiments to study large-scale path loss at 2.4 GHz in the sea port environment. These investigations are useful because it allows us to understand the feasibility of deploying IEEE 802.16 based radios for the mesh network for communication between ship-to-ship and ship-to-shore. From our studies, we discovered that the two-ray model fits measured large scale path loss reasonably well when Line Of Sight (LOS) is dominant. Figure 2 shows the path loss measurement in the 2.4 GHz band when the transmitter antenna was placed on top of a 76 m lighthouse. In this measurement setting, the LOS condition was dominant.

In Figure 2, the dots represent measured mean received power while the boat was making way. The normalized distance log (d/d_0), where $d_0 = 10$ m, includes the lighthouse's height. The curve that has peaks and nulls is the calculated received power using two-ray model at normalized distance of the data. Because the sea surface at 2.4 GHz satisfies a good conductor condition, the two ray model fits closely with the measured data and fully explains the propagation characteristics observed. The path loss exponent is found to be 2.09 and the standard deviation is 6.43 dB. During our experiment, when Non Line of Sight (NLOS) occurred due to blockage of larger ships, received power could drop by 20 dB. In another study where the objective was to emulate lower angled transmissions between ships, we placed a transmitter antenna on a tripod at about 5.25 m from the sea level. Although it is uncommon to use two-ray model when LOS is not dominant [6], we found that it is useful to estimate the break point to calculate path loss exponents and their respective standard deviations using double regression satisfying Minimum Mean Square Error (MMSE). Figure 3 shows double regression results with Minimum Mean Square Error (MMSE) constraint when the boat was making way and using d_A (obtained from two-ray model) as the break point. The path loss exponent n_1 and n_2 are 2.16 and 4.69, respectively. Their respective standard deviations are 2.42 and 7.9 dB.

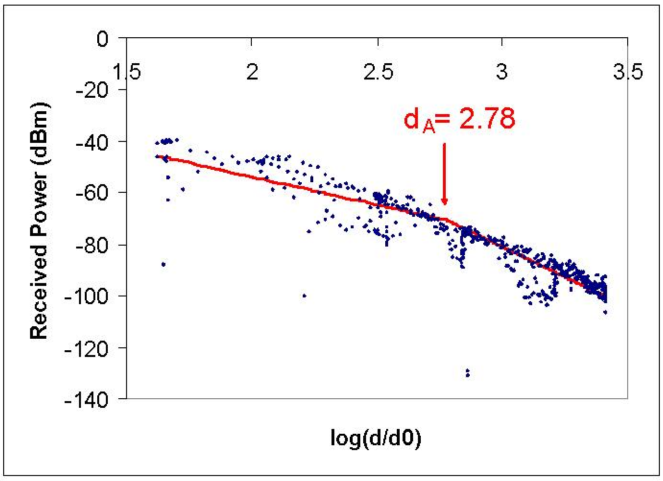

Figure 3. Path loss exponent when TX at 5.25 m

For the second experiment, when $d < d_A$, the path loss exponent is closed to that of free space, which is equal to 2. However, when $d > d_A$, the path loss exponent is slightly larger than that predicted by the two ray model, which is equal to 4. Similar observation was made for the case of 5.8 GHz [4]. A larger path loss exponent could be due to the fact that beyond d_A, direct path and reflected path are grazing sea surface (which is not stationary). Because path loss exponent is very large beyond d_A, the signal will attenuate very rapidly and this will limit the coverage zone of WiMAX. The performance of WiMAX 802.16d radio has also been studied by our group and reported in [4]. Based on the above measurements and the studies carried in [4], we believe that mesh links using WiMAX radios are feasible because the general propagation follows a two-ray model with path loss exponents close to those applicable to urban and rural areas. In designing the radios, we also need a proper networking layer to help establish alternative routes when there is significant drop in received signal strength due to ship blockage or nulls due to reflection of sea surface.

IV. Connectivity analysis

In the maritime environment, ships move in an autonomous way but are confined to traffic lanes. In TRITON system, each node can function as a relay station for routing traffic to its final destination. Providing a given level of QoS to users depends on the maintenance of the best connectivity level. The increase of the connectivity will then increase the QoS level in terms of ensuring continuity of communication, failure backup and load balancing. From a practical point of view, connectivity is a prerequisite to providing reliable applications to the users of a wireless multi-hop maritime communication network. In the literature, there is no existing connectivity studies carried out for the maritime communication environment. In view of this, we performed a detailed connectivity analysis for a maritime communication network. The analysis is unique because it is based on actual mobility traces of ship derived from AIS data observed in a specific region. The region of interest is shown in Figure 4, which is a rectangular area close to the East Coast of Singapore. The north east corner of the region is located at latitude is 1.333 and longitude 104.167. The south west corner of the region is located at latitude 1.183 and longitude 103.850.

Figure 4. Region of interest - East Coast of Singapore

From the analysis, a high level of connectivity in the presence of actual ship mobility can help in confirming the feasibility of TRITON architecture presented earlier in Figure 1. In this connectivity study, we only consider a topology based scheme, which does not consider interference. Therefore, two nodes are considered connected if they are within transmission range of each other. In this study, we consider the network model as shown in Figure 1, which is a generalized form of the maritime mesh network architecture. From this model, we consider the communication between ships and the land station, which is connected to the terrestrial network. To achieve a fully connected network, there must be at least one path between each ship to the land station. The path between a ship and the land station may consist of one hop (when they are neighbors) or several hops (when ships relay packets for other ships). When there is no path between at least one ship-land-station pair the network is said to be disconnected. By varying the radio range between the base station (BS) and a subscriber station (SS), i.e, the BS-SS radio range, and radio range between two subscriber stations, i.e., the SS-SS radio range, we study the connectivity that could be achieved.

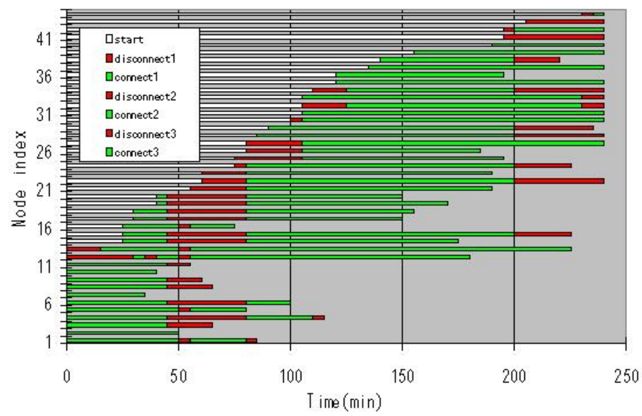

Figure 5. Connectivity with BS-SS range of 10 km and SS-SS range of 8 km

Figure 5 gives a view of the connectivity of 44 ships over a period of time when the BS-SS and SS-SS radio ranges are set to 10 km and 8 km, respectively. The figure shows that for a SS to SS radio range of 8 km, there can be periods of up to 40 minutes with disconnection. Intuitively, we can observe that connectivity can be improved if the SS-SS and BS-SS radio ranges are increased. However, due to limited experimental data from actual IEEE 802.16 mesh radio at the moment, we are unable to determine the actual maximum distances for which the radio is able to operate at. Physical propagation conditions, atmospheric conditions, frequency, sea-states, modulation techniques, etc. will eventually determine the maximum distance possible. Due to this reason, we will study the connectivity for a range of distances of between 8 km to 20 km. The connectivity study is useful since it helps us derive the inter-base station distances to use and the minimum mesh radio link distance that should be used for ship-to-ship communications. Another characteristic that is critical for the study of connectivity and dimensioning of the inter-base station distance is the mobility pattern of the ships. If ships are uniformly spaced and within the radio range of each other, then we can safely assume that ships will be connected at all times. However, as shown in the next section, the ship movement pattern is somewhat random and clustered at times but with consistent inter-arrival and speed distributions.

Besides the connectivity study, we studied the route redundancy from the AIS data to study the possibility of using multi-path routing to achieve high transport reliability. In multi-path routing, if one route fails temporarily, another route can be used to quickly forward packets. In the study, we compute the number of node disjoint paths from any given node to the BS, including one-hop, two-hop and three-hop path. The route redundancy with BS-SS and SS-SS ranges of 10 km is shown in Figure 6. In the figure, the different shaded area of the bar represents the numbers of 1-hop, 2-hop and 3-hop routes, respectively. Similar to the connectivity study, we observed that with the larger transmission range between two SS, the number of node-disjoint routes increases and thus improve the transport reliability. The study of both connectivity and route redundancy, in relation to ship mobility is still in progress and will be reported in future publications related to the TRITON project.

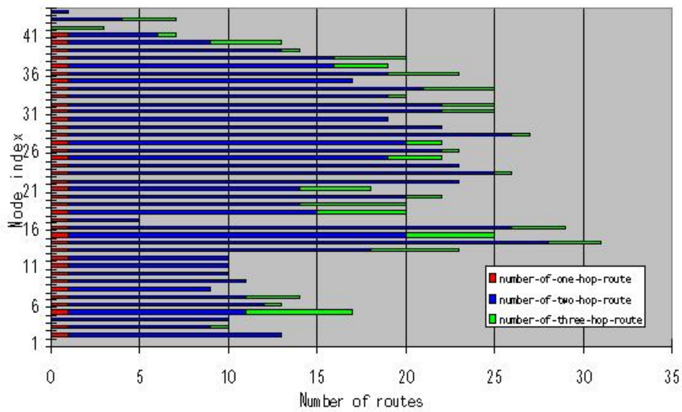

Figure 6. Route redundancy with BS-SS range of 10 km and SS-SS range of 10 km

V. SHIP MOBILITY PATTERN

In the previous sections, studies were carried out to give us an indication on the general feasibility of carrying out the multi-hop transmission and also derive valuable connectivity information based on possible radio ranges between nodes. We also studied route redundancy to establish the type of routing protocols that can be used in our system. To further help us in determining the inter-base stations distances, we have to consider the mobility pattern of the ships. This section details the analysis of the mobility pattern. We have extensively analyzed the AIS data provided by MPA (Maritime and Port Authority of Singapore) to determine the mobility pattern of ships traveling in the Singapore Straits. Besides aiding in the dimensioning of the network, the mobility pattern will also be used in the maritime network simulator that we have developed. The maritime simulator will be used to design suitable networking protocols for the TRITON system.

We focus on analyzing the distributions of inter-arrival times and speeds of all ships crossing a given liner line on earth surface. Figures 7 and 8 show the number of ships that cross the vertical line at longitude 140.15 hourly heading west and east. The figures show that there is no obvious trend in hourly distribution. Also, there is no obvious difference in the ship arrival patterns of both directions. The total numbers of ships heading west and east in the 24-hour periods are 151 and 146, respectively.

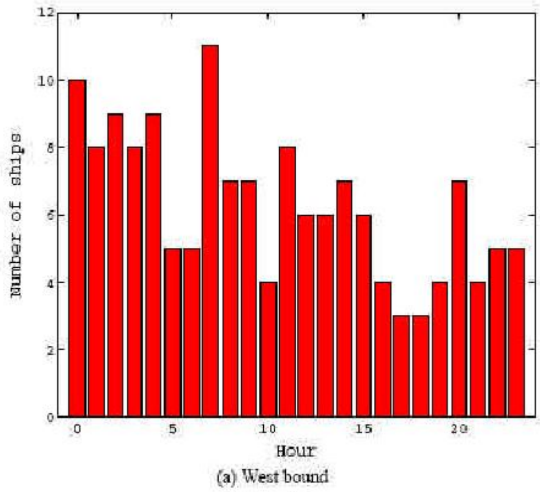

Figure 7. The number of ships that cross longitude 140.15 hourly in west bound direction

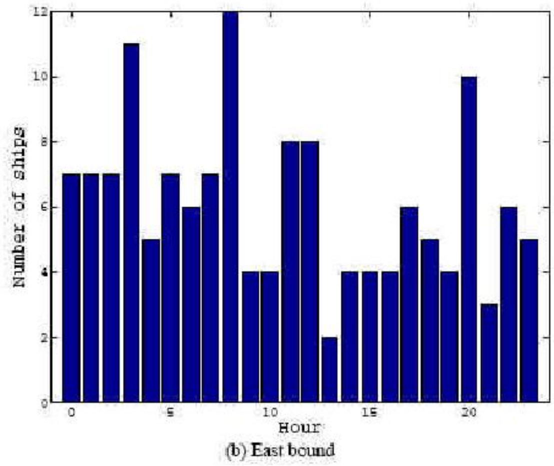

Figure 8. The number of ships that cross longitude 140.15 hourly in east bound direction

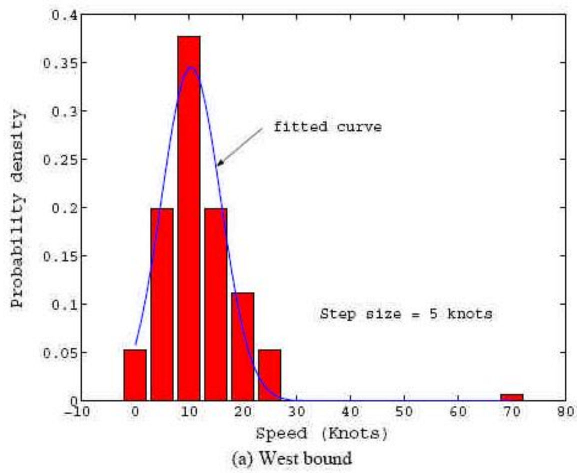

Figure 9. The speeds of ships that cross longitude 140.15 in west bound direction

Figures 9 and 10 show the probability density functions of the speeds of ships that cross the linear line at longitude 140.15. We observed that there is no obvious difference in the speed distributions of both directions. Majority of the speeds are under 30 knots, which is the maximum speed allowed in the shipping lane and ships in the port area are expected to move slower. The outliers at about 70 knots are probably due to errors in the AIS data.

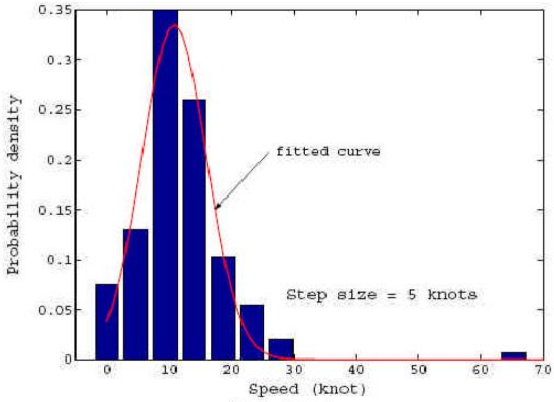

(b) East bound

Figure 10. The speeds of ships that cross longitude 140.15 in east bound direction

By using commercially available curve fitting software, DataFit [7], we manage to perform non-linear regression to fit the probability density functions of speeds in Figure 9 into a factorized truncated normal function with the following form:

$$p(x) = \frac{c}{\sqrt{2\pi\sigma^2}} e^{-(x-\mu)^2/(2\sigma^2)}, \tag{1}$$

where x is the speed, c is the multiplicative factor, μ is the mean value, and σ is the standard deviation. However, p(x) above is not ready for use as the probability density function and we need to first ensure the compliance with probability conservation rule. Let *P(x)* be defined as follows:

$$P(x) = \int_{-\infty}^{x} \frac{c}{\sqrt{2\pi\sigma^2}} e^{-(y-\mu)^2/(2\sigma^2)} dy. \tag{2}$$

Then, the speed probability distribution function for a given c, μ and σ can be written as follows:

$$F(x) = \begin{cases} \dfrac{P(x) - P(0)}{P(70) - P(0)} & \text{if } 0 < x \le 70, \\ 0 & \text{otherwise,} \end{cases} \tag{3}$$

where P(70) is used in the denominator as a result of the observed maximum speed 70 knots. The speed of a new arrived ship is determined using the F(x) in equation (3) derived above.

Figures 11 and 12 show the probability density functions of the inter-arrival times of all ships that cross the liner line at longitude 140.15. Similarly, there is no obvious difference in the inter-arrival time distribution in both directions. In both cases, arrivals of more than 60% of the ships are separated by an interval of up to 400 seconds.

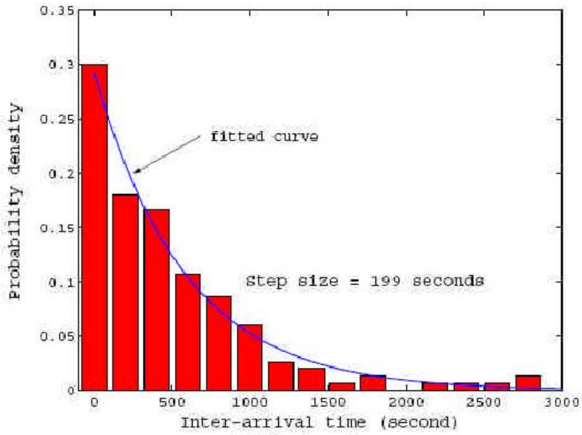

(a) West bound

Figure 11. The inter-arrival times of ship that cross longitude 140.15 in west bound direction

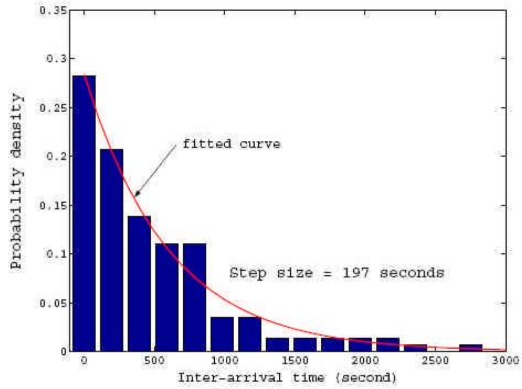

(b) East bound

Figure 12. The inter-arrival times of ship that cross longitude 140.15 in east bound direction

We could not fit Figure 11 into a form of exponential distribution using DataFit [7]. Instead, we manage to produce fits for the following ‘‘not well known’’ functions:

$$p(x) = a \times b^x, \tag{4}$$

where x is the inter-arrival time, and both a and b are arbitrary factors. For Figure 11, a = 0.292064 and b = 0.998286. For Figure 12, a = 0.284495 and b = 0.998324. Let P(x) be defined as follows:

$$P(x) = \int_{-\infty}^{x} a \times b^y dy. \tag{5}$$

Then, the inter-arrival time probability distribution function for a given a and b can be written as follows:

$$F(x) = \begin{cases} \dfrac{P(x) - P(0)}{P(3000) - P(0)} & \text{if } 0 < x \le 3000, \\ 0 & \text{otherwise,} \end{cases} \tag{6}$$

where P(3000) is used in the denominator as a result of the observed maximum inter-arrival time 3000 seconds. The interval to the next new ship arrival, i.e., the ship inter-arrival time is determined using the F(x) derived in equation (6) above.

VI. Maritiime Simulator

The maritime network simulator provides detailed modeling to a few unique aspects of a maritime communication network. Specifically, it has a topology that represents a generic busy narrow navigation channel. For this topology, the nodes are either static land stations that are installed on land or mobile ships sailing in the shipping lane. Based on equations (3) and (6), which describes the mobility model in Singapore Straits, we have written a function generate the ships arrival pattern for the generic topology. In addition, the simulator also models the random movement of sea surface and the radio propagation in a maritime environment. The radio propagation model adopted in the simulator is based on our measurement and observation. We have also develop a simulation model for IEEE 802.16-2004 mesh MAC because we are currently keen in exploring the use of IEEE 802.16 for its longer transmission range and larger coverage. The entire maritime network simulator is developed on QualNet 3.9.5 [8].

VII. Conclusion

In this paper, we describe an ongoing project known as TRITON that aims to develop a high-speed ship-to-ship/shore mesh network. We presented a series of studies that form a systematic approach to studying and establishing the feasibility of developing a multi-hop communication system for ships. The project is still in progress and there are still ongoing efforts to develop the mesh radio, the switching middleware and the suite of networking protocols to form the robust and efficient end-to-end quality of service framework for the mesh network.

References

[1] www. fleet.inmarsat.com

[2] H. L. Bertoni, Radio Propagation for Modern Wireless Systems. New Jersey: Prentice Hall, 1999.

[3] J An, “Empirical analyses on maritime radio propagation”, IEEE VTC-Spring, May 2004.

[4] J Jurianto. S K Hazra, S H Toh, W M L Tan, J S Pathmasuntharam, M Fujise, “Path Loss Measurements in Sea Port for WiMAX”, IEEE Wireless Communications and Networking Conf., March 2007.

[5] M Zhou, J Jurianto, J S Pathmasuntharam., M Fujise, “Characterization of Radio Path Loss in Seaport Environment for WiMAX Applications”, ISAP, Nov 2006.

[6] T. S. Rappaport, Wireless Communications Principles and Practice. Upper Saddle River, NJ: Prentice-Hall Inc., 2002, pp. 120-126.

[7] www.oakdaleengr.com

[8] www.scalable-networks.com